# Reports

## Laser-Selective Demagnetization: A New Technique in Paleomagnetism and Rock Magnetism

PAUL R. RENNE AND TULLIS C. ONSTOTT

**Laser-selective demagnetization (LSD) enables the determination of the magnetic moment associated with individual mineral grains in thin sections of rock. Small volumes can be demagnetized with laser pulses directed through the optics of a microscope, permitting resolution of remanence components in individual mineral grains. LSD of mafic granulite samples revealed two paleomagnetic directional components of opposite polarity: one resided in coarse magnetite, the other in ilmenohematite-hemoilmenite exsolution intergrowths and fine magnetite inclusions in clinopyroxene. These directions are consistent with those inferred from bulk demagnetization techniques, but LSD permits direct identification of the remanence carriers. The ability to discriminate magnetization components in different generations of a single mineral and to define intergrain magnetic moment distributions are significant advantages of LSD.**

INFERENCE OF PALEOMAGNETIC FIELD directions from magnetizations recorded by rocks has historically entailed the magnetic cleaning of bulk specimens (typically 10 to 12 $cm^3$) to isolate discrete components. Thermal and alternating field (AF) demagnetization, the most frequently used techniques for magnetic cleaning (*1*), can be used to resolve multiple magnetic components only if the various magnetic mineral phases have different blocking temperatures or coercivities. Similarly, chemical demagnetization (*2*) exploits differential solubilities of the various minerals, but cannot be used to distinguish between magnetic components carried by different generations of a single phase that have similar solubilities.

To overcome the restrictions of bulk demagnetization, several workers have used microanalytical techniques to analyze specimens of substandard volume, down to the scale of individual mineral grains (*3–5*). These techniques have proven to be useful adjuncts to bulk demagnetization methods in solving geologic, paleomagnetic, and rock magnetic problems (*6*), but are difficult to apply on a routine basis because they require manual extraction and orientation of each grain to be analyzed.

We have developed a laser-selective demagnetization (LSD) technique for the measurement of the magnetic moment associated with individual mineral grains and thus the determination of distinct components of paleomagnetism carried by grains that have similar blocking temperatures, coercivities, and solubilities. This technique allows thin sections to be used and is much less laborious than other microanalytical methods.

We analyzed specimens of a medium-grained basic granulite from the El Pao iron mine in the Imataca Complex of the Guiana Shield, Venezuela, to test LSD. The granulite contains clinopyroxene, orthopyroxene, plagioclase, hornblende, magnetite, and composite oxide grains that consist of exsolved intergrowths of hemoilmenite, ilmenohematite, corundum, and hercynite (Fig. 1A). The clinopyroxene contains crystallographically oriented magnetite rods (Fig. 1B) averaging about 10 to 50 μm long and about 1 to 2 μm in diameter. Electron microprobe analysis indicates that no detectable Ti is in the rods. The origin of these rods is uncertain, but they are common in high-grade metamorphic rocks (*7*). Dating of this and nearby rock units with $^{40}Ar$-$^{39}Ar$ methods (*8, 9*) and petrologic studies (*10*) indicate that the Imataca Complex cooled slowly (approximately 5° to 10°C per million years) following granulite facies metamorphism 2.0 billion years ago. Protracted cooling apparently facilitated the extensive exsolution and development of retrograde mineral assemblages observed in the rock.

Thermal and AF demagnetization of bulk (11 $cm^3$) specimens revealed that they possess multiple components of magnetization (Fig. 2). All specimens have a shallow north-northwest directional component (A) that dominates the natural remanent magnetization and was thermally unblocked discretely between 540° and 560°C; a second, approximately antipolar component (B) was evident at higher temperatures. Progressive AF demagnetization shows that component A has lower coercivity than component B, so that higher peak demagnetizing fields produced composite directions progressively displaced along a great circle (in stereographic projection) toward component B. In many specimens, a stable endpoint defining either the A or the B component was not isolated with either thermal or AF demagnetization.

The relative intensities, coercivities, and unblocking temperatures of components A and B generally suggest that A is associated with magnetite and B with ilmenohematite. The contributions to the A component from various observed paragenetically distinct magnetite grains (for example, rods in pyroxene or discrete grains) was uncertain from bulk demagnetization data. Antipolarity of the B component with respect to the A component was presumably caused by either (i) self-reversal in an A-oriented field (*11*) or (ii) magnetic blocking of this phase at a different time, during which the geomagnetic field was of opposite polarity. The A component is similar to paleomagnetic directions obtained from igneous and high-grade metamorphic rocks throughout the Imataca Complex; its acquisition age is probably close to 1.95 billion years ago, the

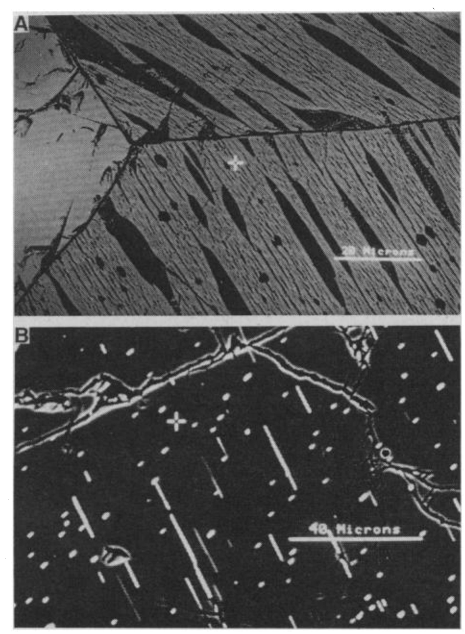


**Fig. 1.** (**A**) Backscattered electron image of two exsolved rhombohedral oxide grains (striped) and a homogeneous magnetite grain (left). Lighter lamellae are ilmenohematite; darker lamellae are hemoilmenite. Dark equant spots less than 5 μm in diameter are corundum. Scale bar is 20 μm. (**B**) Backscattered electron image of magnetite rods (white) in clinopyroxene (dark). Note two distinct orientations of the rods, parallel to and nearly perpendicular to the image plane. Black features are cracks in the clinopyroxene. Scale bar is 40 μm.

Department of Geological and Geophysical Sciences, Princeton University, Princeton, NJ 08544.

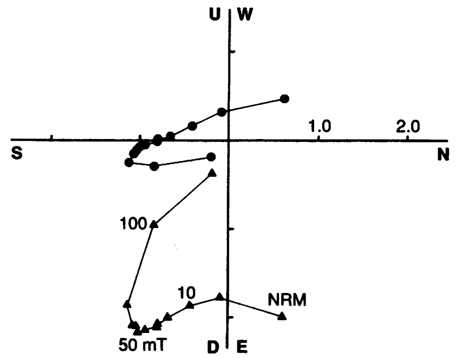


**Fig. 2.** Orthogonal demagnetization diagram (*1*) depicting the results of AF demagnetization on bulk sample 28-1. Circles represent the end points of magnetization vectors (units of magnitude are amperes per meter) projected onto a horizontal plane; triangles represent projections onto a north-south vertical plane (U is up). The peak demagnetizing field in millitesla (mT) is shown for some measurements. NRM, natural remanent magnetization. The vectors do not decay to the origin, indicating that the high-coercivity B component has not been isolated by 120 mT.

$^{40}Ar$-$^{39}Ar$ plateau date on hornblende separated from these samples (*9*).

We selectively demagnetized oriented specimens (*12*) with pulses from a ruby laser, supplying approximately 100 to 200 J of energy instantaneously to the specimen through the optical system of a metallurgical microscope (*13*). The microscope was placed in a mu-metal box of about 0.06 $m^3$ that was open at the top to reduce ambient magnetic fields and to minimize possible effects of electromagnetic pulses from the laser power supply on the magnetization of the specimens. A gaussmeter probe placed inside the box registered no magnetic pulse upon discharge of the laser power supply.

One to 35 laser pulses were directed into 41 individual mineral grains in five specimens prepared from two different oriented cores. Each pulse produced a fusion crater, or "pit," approximately 50 to 150 μm in diameter (Fig. 3). Pit dimensions and morphology are obscured by melt glass in Fig. 3, but they are circular at the surface and in some cases penetrate through the specimen. The volume of sample that was demagnetized thermally by each pulse is not known, but was probably not significantly greater than the pit volume (*14*). The mode of demagnetization affected by LSD is thus a combination of selective destructive demagnetization (*4*) and thermal demagnetization.

We measured the magnetization of specimens before and after each suite of pits was emplaced; the demagnetizing effect of each suite was calculated by vector difference. Natural remanent magnetization intensities of individual specimens before applying LSD ranged from $10^{-8}$ to $10^{-10}$ A-$m^2$. Magnetizations were measured with a two-axis cryogenic magnetometer; the noise level (determined by replicate measurements) was less than $5 \times 10^{-11}$ A-$m^2$.

The total magnetic moment associated with each suite of demagnetizing pulses ranged from $3 \times 10^{-10}$ to $8 \times 10^{-9}$ A-$m^{-2}$. The mean change in magnetization intensity per laser pulse (*J/P*) was highest for magnetite grains (Table 1), followed by rhombohedral oxides, and then clinopyroxenes. Variability in *J/P* (for different measurements) for each grain type probably reflects variable demagnetization volumes and varying crystallographic orientations of the grains with respect to the original magnetizing field. Another likely source of variation in *J/P* for the rhombohedral oxide and clinopyroxene grains is the inherently inhomogeneous distribution in each of these composite phases of the material that is actually magnetic (presumably ilmenohematite in the rhombohedral oxides and magnetite in the clinopyroxenes). The width of exsolution lamellae in the rhombohedral oxides is variable but generally smaller than the diameter of laser pits (Fig. 3). Impingement of the laser beam on magnetite grains beneath the specimen surface, hence undetectable in reflected light, apparently caused several measurements of anomalously high intensity from clinopyroxenes.

**Table 1.** Summary of LSD and bulk sample paleomagnetic directions. M, coarse-grained magnetite; $R_1$ and $R_2$, ilmenohematite-hemoilmenite composite grains; C, clinopyroxene grains with included magnetite rods. Data from AF demagnetization of bulk (11-$cm^3$ volume) specimens are from the same site. Also shown is the mean Nickorie overprint (NO) direction pooled from different sites in the Imataca Complex; Dec is declination and Inc is inclination of the mean vector (in degrees); *N* is the number of grains for LSD data, the number of specimens for site ON-28 bulk results, and the number of sites for NO direction; negative inclination refers to an upward direction; *k* is an unbiased estimate of Fisher's precision parameter (*16*); $\alpha_{95}$ is the radius of the 95% confidence interval (in degrees), *J/P* is the magnetic moment removed per laser pit, in units of $10^{-9}$ amperes per meter squared per pit ± 1 standard deviation in parentheses.

| Sample | *N* | Dec | Inc | *k* | $\alpha_{95}$ | *J/P* |
|---|---|---|---|---|---|---|
| | | | *Core 28-1 LSD* | | | |
| M | 7 | 343.6 | 7.4 | 6.3 | 21.1 | |
| $R_1$ | 10 | 134.5 | −26.3 | 5.1 | 19.6 | |
| $R_2$ | 4 | 57.7 | 13.1 | 44.6 | 10.5 | |
| C | 12 | 141.6 | 9.7 | 3.8 | 20.6 | |
| | | | *Core 28-2 LSD* | | | |
| M | 3 | 353.1 | 37.9 | 29.7 | 14.8 | |
| $R_1$ | 3 | 135.8 | 19.7 | 3.5 | 43.2 | |
| $R_2$ | 2 | 68.2 | −24.3 | 5.8 | 41.1 | |
| | | | *Combined LSD* | | | |
| M | 10 | 346.3 | 16.5 | 7.5 | 16.1 | 0.94 (0.64) |
| $R_1$ | 13 | 151.0 | −13.7 | 2.3 | 22.9 | 0.58 (0.31) |
| $R_2$ | 6 | 60.9 | 1.4 | 11.4 | 16.9 | 0.38 (0.11) |
| C | 12 | 141.6 | 9.7 | 3.8 | 20.6 | 0.09 (0.07) |
| | | | *Bulk demagnetization* | | | |
| ON-28 | 7 | 341.9 | −29.3 | 81.0 | 7.3 | |
| NO | 7 | 67.4 | 5.3 | 6.4 | 20.9 | |

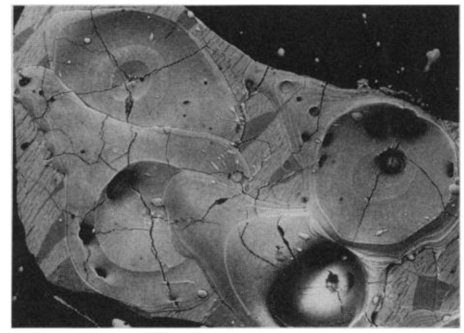

**Fig. 3.** Scanning electron photomicrograph, made with mixed secondary and backscattered electron images, of several laser pits in a composite rhombohedral oxide grain. Exsolution lamellae of ilmenohematite (light) and hemoilmenite (dark) give the grain its banded appearance. Field of view is 400 μm.

The directions of magnetization (Fig. 4 and Table 1) measured from discrete magnetite (component M) and composite rhombohedral oxide grains (component $R_1$) in specimens from the two independently oriented cores define two antipolar directional modes. These directions lie nearly 180° apart on the great circle distribution defined by composite directions revealed in progressive AF demagnetization. Six grains of composite rhombohedral oxide yielded directions (component $R_2$) that define a second bipolar cluster (Fig. 4) with northeast or southwest declination and shallow inclination. Grains bearing the $R_2$ direction were physically and optically similar to those bearing the more typical southeast direction; their anomalous directions are discussed below. The directions associated with clinopyroxene (component C) are more dispersed than directions from other grains (Fig. 4). Those with weaker intensities are much better clustered, which suggests that contamination by discrete grains of magnetite having opposite polarity most likely is the source of some of the scatter. The C directions associated with anomalously high intensity are significantly displaced toward the magnetite directional mean along apparently random trajectories, as would be expected for linear combinations of statistically antipolar but variable vector distributions. The directions associated with *J/P* values greater than 3 standard deviations from the mean for clinopyroxene grains were thus excluded from the data shown in Table 1.

The M and $R_1$ magnetization directions determined by LSD are generally consistent with the results of bulk demagnetization

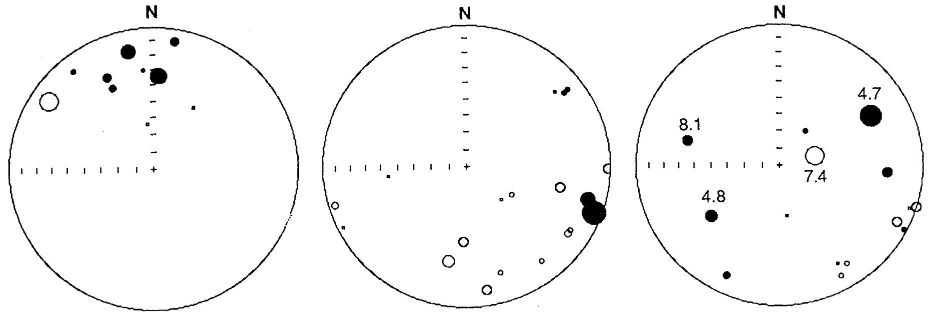


**Fig. 4.** Equal area stereographic projections of paleomagnetic directions for different grain types, in geographic coordinates (restored to field orientation). Open symbols are in the upper hemisphere (negative inclination). Size of symbols is proportional to magnetization intensity. Numbered symbols in right plot correspond to measurements of anomalously intense magnetization, discussed in the text.

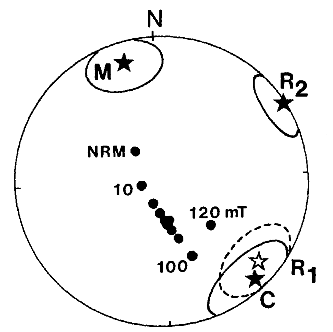


**Fig. 5.** Comparison of LSD-derived directions with results of AF demagnetization (filled circles) of bulk specimen 28-1 (equal area stereographic projection). Solid symbols are in the lower hemisphere; M, $R_1$, $R_2$, and C are mean magnetization directions (see text) from magnetite, rhombohedral oxides, and pyroxene (with included magnetite) grains. Ellipses are 95% confidence intervals, dashed in the upper hemisphere. Peak demagnetizing field in millitesla (mT) is shown for some of the AF measurements.

data (Fig. 5) but are determined less precisely than the site mean A direction (Table 1). Although the mean LSD directions from the two cores are statistically indistinguishable, the small number of analyses from sample 28-2 precludes rigorous comparison between the two populations. An alternative test for homogeneity of intergrain results between different core samples involves estimating the dispersion at the site level that would arise solely from the observed intergrain dispersion and comparing the result with the site mean dispersion determined from bulk demagnetization data. We employed a two-tiered Monte Carlo simulation (*15*) to generate and add synthetic Fisher distributions (*16*) with precision parameters ($k$) given by the M, $R_1$ and C components from sample 28-1. Each distribution comprised a number of unit vectors determined by an estimation of the number of grains (*17*) of the appropriate mineral in 11 $cm^3$ of rock. The average of seven modeled bulk specimens yielded site mean values of $k$ from around 800 for $R_1$ to greater than 10,000 for M and C. From this comparison, we conclude that other factors (for example, heterogeneity of mean directions or dispersion) in addition to intergrain dispersion must have produced the much larger observed site mean dispersion ($k$ = 81) for the A (analogous to M) component.

The expected intergrain dispersion for randomly oriented grains in a uniform magnetic field depends on the strength of the magnetizing field, magnetic domain structure of the grains, and thermal history during acquisition of magnetization (*1*). Additional dispersion should occur if individual grains acquire their magnetization at various times during an interval long enough for significant secular variation of the geomagnetic field to occur; magnetization of an ensemble of single-domain magnetite grains may have taken 2 to 3 million years in the Imataca Complex (*18*). Intergrain precision parameters for the four mineralogical directional components are less than but close to the value of 18.5 predicted (*19*) for dispersion of the geomagnetic field direction due to secular variation at the paleolatitude (5.2°) corresponding to the mean inclination of the four components.

Low signal to noise ratio and the unknown effects of laser pulses on intracrystalline magnetic domain structure may also have contributed to apparent directional scatter in the data. Specimen orientation errors may have introduced some variance, but this would be primarily azimuthal in specimen coordinates, a feature not apparent in the data. Further LSD experiments on quickly cooled rocks, which should show little or no dispersion resulting from secular variation, will be needed to resolve the relative contributions of experimental error and real, geologically meaningful variation. Confidence intervals ($\alpha_{95}$) about the LSD mean directions can be decreased by simply demagnetizing more grains; for example that of the M component could be decreased from 16.1° to 5.0° by analyzing 123 rather than 10 grains.

Anomalous northeast-southwest directions ($R_2$) associated with six composite rhombohedral oxide grains (Fig. 5) are similar in orientation and bipolarity to secondary directions encountered throughout the Imataca Complex (*20*) that were acquired during the Nickorie episode, a low-grade thermal event manifested by a 1.2-billion year $^{40}Ar$-$^{39}Ar$ plateau date on plagioclase from one of the samples used in this study, and on other feldspar samples from throughout the Imataca Complex (*9*). Why only some grains were affected during the Nickorie episode is unknown, but the broad range in the scale and composition of exsolution products may have produced a corresponding range of effective coercivities and blocking temperatures, hence susceptibility to remagnetization.

Some specific results obtained from the application of LSD, not readily deduced from bulk demagnetization, include the observations that: (i) two paragenetically distinct magnetite populations are associated with antipolar components; (ii) ilmenohematite is also associated with two components, one of which is probably a low-temperature overprint; (iii) the apparent intergrain directional dispersion is much higher than interspecimen dispersion, but is much lower than required in a two-level hierarchical sampling scheme to account solely for the site mean dispersion if the mean directions, dispersion, and mineralogical abundances are homogeneous throughout the site; (iv) the antipolarity of the M and C magnetite components suggests that $R_1$ may have been acquired in a C-oriented field rather than being self-reversed in an M-oriented field.

Combined with results from other microanalytical techniques, such as geothermometry from electron microprobe data and thermochronometry from $^{40}Ar$-$^{39}Ar$ laser probe or ion microprobe data, LSD of a single thin section could provide information on, for example, apparent polar wander path segments or geomagnetic reversal frequency. Rock magnetic inquiries concerned with populations of individual grains could benefit from application of LSD, as might studies limited to small samples as in the field of extraterrestrial magnetism.

REFERENCES AND NOTES

1. J. A. As and J. D. A. Zijderfeld, *Geophys. J. R. Astron. Soc.* **1**, 308 (1958); F. D. Stacey and S. K. Banerjee, *The Physical Principles of Rock Magnetism* (Elsevier, Amsterdam, 1974).
2. D. W. Collinson, in *Methods in Paleomagnetism*, D. W. Collinson, K. M. Creer, S. K. Runcorn, Eds. (Elsevier, New York, 1967), pp. 306–310.
3. Y. T. Wu, M. Fuller, V. A. Schmidt, *Earth Planet. Sci. Lett.* **25**, 275 (1974); K. L. Buchan, *Can. J.*

Earth Sci. 16, 1558 (1979); G. M. Smith, *Earth Planet. Sci. Lett.* 78, 315 (1986).
4. E. E. Larson, *Geology* 9, 350 (1981).
5. J. W. Geissman, *J. Geophys. Res.* 85, 1487 (1980).
6. An informative review of these techniques and their use in conjunction with electron microscopy is given by J. W. Geissman, S. S. Harlan, A. J. Brearly [*Geophys. Res. Lett.* 15, 479 (1988)].
7. M. F. Fleet *et al.*, *Can. Mineral.* 18, 89 (1980).
8. T. C. Onstott, R. B. Hargraves, D. York, C. Hall, *Geol. Soc. Am. Bull.* 95, 1045 (1984).
9. T. C. Onstott *et al.*, *Precamb. Res.*, in press.
10. S. M. Swapp and T. C. Onstott, *ibid.*, in press.
11. The possibility that certain compositions of Ti-hematite may be self-reversing has been noted in several studies, including J. R. Balsley and A. F. Buddington, *J. Geomagn. Geoelectr.* 6, 176 (1954); R. B. Hargraves and D. M. Burt, *Can. J. Earth Sci.* 4, 357 (1967); R. T. Merrill and C. S. Gromme, *J. Geophys. Res.* 74, 2014 (1969); C. A. Lawson *et al.*, *Science* 213, 1372 (1981).
12. Specimens were prepared from polished wafers 200 to 300 μm thick cut from oriented cylindrical cores 2.5 cm in diameter and mounted with epoxy on glass slides. Parallel scribe lines approximately 2 to 4 mm apart were scored on the wafers with a diamond-tipped carbide scribe to permit orientation. Oriented discs were then drilled from the wafer with a water-cooled drill press and 3- to 5-mm-diameter drill bits tipped with diamond-impregnated brass alloy. We obtained specimens smaller than the drill diameter by drilling near the edge of the wafer. The specimens along with their glass substrates were then glued onto 2.5-cm-diameter circular glass slides. A fiducial mark scored radially from the specimen to the edge of the slide facilitated rapid orientation of the specimen in the magnetometer.
13. The binocular microscope has reflected light illumination and ×4, ×10, and ×20 objectives, enabling the user to make routine optical observations and identification of opaque minerals. The laser beam alignment is adjustable, so that precise coincidence of the beam with microscope cross-hairs is easily attained; this laser-microscope instrument was described by T. Plieninger and O. A. Schaeffer [*Proc. Lunar Sci. Conf.* 7, 2055 (1976)].
14. Data from laser-probe $^{40}Ar$-$^{39}Ar$ dating [for example, D. Phillips and T. C. Onstott, *Geology* 16, 542 (1988)] indicate that ferromagnesian silicate grains are not heated above approximately 300°C farther than 20 μm from the edges of similar laser pits.
15. The Monte Carlo calculations were made with a modified version of a BASIC program [P. R. Renne, G. R. Scott, A. L. Deino, *Eos* 68, 1251 (1987)]. The algorithm builds a Fisher distribution (*16*) of unit vectors from pairs of random numbers.
16. R. A. Fisher, *Proc. R. Soc. London Ser. A* 217, 295 (1953).
17. We estimated the number of grains per 11-$cm^3$ specimen from modal abundances (*10*) and the maximum observed dimension of each mineral type in thin sections, assuming spherical grain geometry. Using the maximum observed dimension implies a minimum estimate for the number of grains per bulk specimen. Estimated minimum values are 252 grains per specimen for the rhombohedral oxides, 2434 for the clinopyroxenes, and 4324 for discrete magnetite.
18. D. York, *Earth Planet. Sci. Lett.* 39, 94 (1978).
19. P. L. McFadden, *Geophys. J. R. Astron. Soc.* 61, 183 (1980).
20. T. C. Onstott and R. B. Hargraves, *Transactions of Caribbean Geological Conference IX* (Santo Domingo, Dominican Republic, 1980), vol. 2.
21. K. P. Kodama provided access to his cryogenic magnetometer at Lehigh University, assisted in setting up the apparatus, and made many useful suggestions. The laser microscope used for these experiments was loaned by W. D. Sharp. We thank J. A. Stamatakos and G. A. Deamer for assistance in use of the magnetometer laboratory. S. M. Swapp helped obtain electron microprobe analyses and electron backscatter images, partly supported by NSF grant EAR86-18070. E. V. Lenk provided scanning electron microscope photographs. We thank R. B. Hargraves, K. P. Kodama, and G. R. Scott for useful discussions and reviews of the manuscript.

14 July 1988; accepted 29 September 1988

# Genetic Relatedness in Colonies of Tropical Wasps with Multiple Queens

DAVID C. QUELLER, JOAN E. STRASSMANN, COLIN R. HUGHES

**The evolution of worker behavior in the social insects is usually explained by kin selection: although workers do not produce offspring, they do reproduce their genes by aiding the reproduction of relatives. The most difficult case for kin selection theory would be species in which workers are fully capable of reproducing but instead opt to rear brood of low relatedness. These conditions are perhaps best fulfilled by the swarm-founding wasps because they have little caste differentiation and their colonies usually have multiple queens, which should lower relatedness. Estimates of within-colony relatedness for three species in this group confirm that it is sometimes (but not always) very low. Inbreeding is negligible in these species, so the hypothesis that inbreeding may raise relatedness is not supported. The maintenance of worker behavior in such species is a significant challenge for kin selection theory.**

THE SWARM-FOUNDING WASPS OF the neo-tropics are a monophyletic group including some 23 genera (*1*). All are social, with even new colonies being founded by swarms of females rather than lone individuals (*2*). Though they are a very successful group (*3*), they have been the subject of few detailed studies (*4*), probably because of their tropical distribution and because most species enclose their nests in an envelope. They are nevertheless a critical group for understanding social evolution.

As in other social Hymenoptera (ants, bees, and wasps), most females function as workers, rearing the young of others instead of rearing their own young. Hamilton showed that this reproductive sacrifice could be favored by kin selection if, by rearing the young of relatives, workers transmit more copies of their genes to future generations than they would by producing offspring themselves (*5*). Hamilton considered the swarm-founding wasps to present "the most testing difficulty" facing his views on the evolution of insect sociality (*6*). The difficulty arises from the polygynous habits of this group; colonies generally have multiple queens, sometimes even numbering in the hundreds (*7–10*). Polygyny poses a problem because egg laying by multiple queens should lower relatedness within colonies, thus diminishing the genetic payoff available to workers. Why should workers continue to rear relatives of a very low degree instead of producing offspring of their own?

At least four explanations are possible. First, workers may be physically unable to reproduce on their own. This seems likely for workers in polygynous ant species (*11*) because ant workers have morphological specializations that may prevent them from successfully reproducing. But it is less plausible for the swarm-founding wasps because most species show little or no morphological differentiation between workers and queens (*4*). A second possibility is that, although workers may be physically able to reproduce, the ecological advantages of group living may be so large as to outweigh the genetic loss of not raising their own offspring. Third, workers may somehow be able to pick out and aid their closest relatives among the brood. Hamilton himself argued for a fourth hypothesis: that inbreeding may increase relatedness and thereby compensate for the relatedness-lowering effect of polygyny (*6*). Inbreeding seemed plausible for these wasps because of the limited dispersal range of swarms and because tropical habitats may permit nonseasonal, asynchronous rearing of reproductives, which makes mates harder to find outside the natal colony. In addition, some circumstantial evidence suggests that mating may take place on the natal nest (*7*).

Although the problem posed by polygyny has been widely recognized (*12*), neither relatedness nor inbreeding has ever been measured for any swarm-founding wasp. We report estimates for three species (*13*). They were collected in April 1988 at Hato Masaguaral, some 40 km south of Calabozo in the Venezuelan Llanos. We collected *Parachartergus colobopterus* along a 4-km stretch of concrete electrical pylons, *Polybia sericea* from shrubs in a small (60 ha) area of savannah, and *Polybia occidentalis* from trees in various areas spread over 2500 ha of

Department of Biology, Rice University, Houston, TX 77005.